ARTICLES

Twisted Intramolecular Charge Transfer of 2-(4′-*N,N*-Dimethylaminophenyl)pyrido[3,4-d]imidazole in Cyclodextrins: Effect of pH

G. Krishnamoorthy and S. K. Dogra*

Department of Chemistry, Indian Institute of Technology Kanpur, Kanpur-208016, India

Received: August 9, 1999; In Final Form: January 9, 2000

Absorption, fluorescence, and fluorescence excitation spectra of 2-(4′-*N,N*-dimethylaminophenyl)pyrido[3,4-d]imidazole (DMAPPI) have been studied as a function of cyclodextrins (CDxs) and acid concentrations. The above study has revealed that a −NMe$_2$ group enters into the CDx cavity and a pyridoimidazole (PI) ring is present at the interface. The =N$_3$− atom and >NH group of the PI ring are involved in the hydrogen bonding with the water molecule present at the interface and/or with the hydroxyl groups of the CDxs, and the =N$_6$− atom is involved in hydrogen bonding with the bulk water. Two monocations (MC1 and MC3) are present in the S$_0$ state, and MC2 and MC3 are present in the S$_1$ state. MC2 emission is observed when MC1 is excited to the S$_1$ state and involves biprotonic phototautomerism, whereas for the MC3 the emission is not observed from the locally excited state, but observed from the twisted intramolecular charge transfer (TICT) state. Fluorescence band maxima of all the bands are blue shifted and their fluorescence quantum yields are enhanced when DMAPPI is encapsulated in the CDxs cavity. The enhancement and the relative blue shifts observed in the band maxima of the TICT band are larger than those of the normal band.

1. Introduction

Cyclodextrins (CDxs) are cyclic oligosccahrides consisting of six (α-CDx), seven (β-CDx), and eight (γ-CDx) D-glucose residues linked by α-(1→4) bonds, with D-glucose residue in the $^4C_1$ chair conformation. These CDx have shapes such as a truncated cone with a hydrophobic cavity and diameters opening at the primary and secondary hydroxyl faces of the cyclic sugar network. This cavity is capable of complexing hydrophobic organic molecules in aqueous solutions. Since this complexation finds a lot of applications in pharmaceutical chemistry, chemical synthesis, and catalysis,[1−5] as well as provides beautiful models for the study of enzyme analysis,[6] a lot of interest has been developed to understand the structure of the inclusion complexes, using different physical techniques.

It is now well established that the physicochemical properties[7−17] (e.g., electronic absorption, fluorescence, phosphorescence, ^{1}H NMR spectra, etc.) of these guest molecules are varied upon the formation of the inclusion complexes with CDxs. The other property which can be affected by the inclusion complexes is the acid−base chemistry. Although some work[11,18−24] has been carried out in this direction in the S$_0$ state, it is not enough to make some generalization. Similar acid−base studies in the S$_1$ state are very scarce.[25]
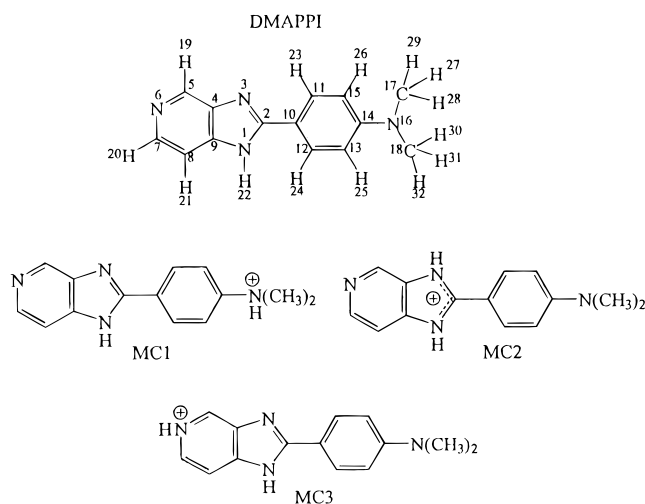
Our laboratory has been active for nearly 2 decades in studying the acid−base properties of the heterocyclic molecules, containing either one or two basic centers.[26] The acid−base chemistry carried out on 2-(4′-aminophenyl, AP), 2-(4′-*N,N*-dimethylamino phenyl, DMAP) benzimidazole[27,28] (BI), benzoxazole[29,30] (BO), and benzothiazole[31,32] (BT) has shown that the formation of the monocations (MCs) by protonating amino or dimethylamino (MC1) or the =N− atom of the imidazole

ring (MC2) in the S$_0$ and S$_1$ states and their relative proportions depend on the benza ring as well as on the polarity of the environments.

We have extended this study to 2-(4′-*N,N*-dimethylaminophenyl)pyrido[3,4-d]imidazole (DMAPPI)[33,34] (Scheme 1). These studies have shown that (i) neutral DMAPPI emits dual fluorescence (locally excited, b and TICT, a state) in polar/protic solvents, (ii) biprotonic phototautomerism is observed between the monocation (MC1) formed by protonating −NMe$_2$ group in the S$_0$ state and the monocation (MC2) formed by protonating =N− moiety of the imidazole ring in the S$_1$ state, and (iii) TICT emission is observed from the monocation (MC3) formed by the protonation of pyrido =N− atom. The relative populations of all the ionic species depend on the polarity of the solvents. Since the polarity of the β-CDx cavity is much less than that of water and β-CDx provides a rigid cavity, it will affect the spectral characteristics of the neutral and the ionic species of DMAPPI. This study thus concentrates on the spectral properties of the neutral and different monocationic species in the presence of β-CDx. Further, this molecule is large in size as compared to the length of β-CDx cavity, this may lead to the formation of either 1:1 complex or 2:1 host−guest inclusion complex. Since the size of the α-CDx is smaller than that of β-CDx, the inclusion complex formed between DMAPPI and the α-CDx may have different photophysical properties when compared with those of the inclusion complex of DMAPPI with β-CDx. We have also carried out the similar studies on DMAPPI with α-CDx.

In most of the studies carried out, the formation of the TICT state has been attributed to the polarity of the medium.[35,36] However, some authors have suggested that the specific

Intramolecular Charge Transfer in Cyclodextrins

J. Phys. Chem. A, Vol. 104, No. 12, 2000 **2543**

SCHEME 1

Figure 1. Absorption spectrum of neutral DMAPPI as a function of (a) α-CDx and (b) β-CDx concentrations.

hydrogen bonding between the solvent and electron donor group also plays a major role to stabilize the twisted conformer and facilitate the formation of the TICT state.[37–39] Kim et al.[40] have recently shown that the hydrogen bonding of the electron acceptor group with solvents stabilized the TICT state and increased its fluorescence intensity in diethylaminobenzoic acid. Such a hydrogen bonding effect may be important in exploring the proton-coupled charge-transfer phenomena often observed in biological assemblies including PS II systems.[41] From this point of view, the investigation of the role of hydrogen bonding on TICT should be extended to other TICT molecules that can be readily hydrogen bonded with solvents. Our earlier studies[33] on DMAPPI indicated that the hydrogen bonding with the acceptor group (pyridoimidazole, PI ring) makes it more planar with benzene ring thereby increases the charge flow and thus enhances its TICT emission. On the other hand, we are not sure about the role of hydrogen bonding of the donor (−NMe₂) group in the formation of TICT state in DMAPPI. Encapsulation of either donor or acceptor by CDx may lead to the conclusion about the role of the hydrogen bonding of the solvent with the donor in the formation of the TICT state.

2. Materials and Methods

DMAPPI was prepared from 3,4-diaminopyridine and *p*-(*N*,*N*-dimethylamino) benzoic acid by the procedure reported in the literature.[42] The compound was purified by repeated crystallization from aqueous methanol. The purity was checked by TLC and verifying that the fluorescence excitation spectrum in cyclohexane was identical when emission was monitored at different wavelengths. CDxs were obtained from Aldrich chemical company (U.K.) and were used as received. Triply distilled water was used for aqueous study. The pH of the solutions in the range 4−9.5 were adjusted by adding small amounts of NaOH or H₂SO₄. The instruments used to record absorption, fluorescence, and fluorescence excitation spectra and to determine the lifetimes and the procedure used to determine fluorescence quantum yield (ϕ_{fl}) have been described elsewhere.[30,33]

3. Results and Discussion

3.1. Spectral Characteristics of the Neutral Molecule. *3.1.1 Absorption Spectrum.* Parts a and b of Figure 1 depict the effect of α-CDx and β-CDx on the absorption spectrum of DMAPPI respectively at pH 9.5. The relevant data along with similar data
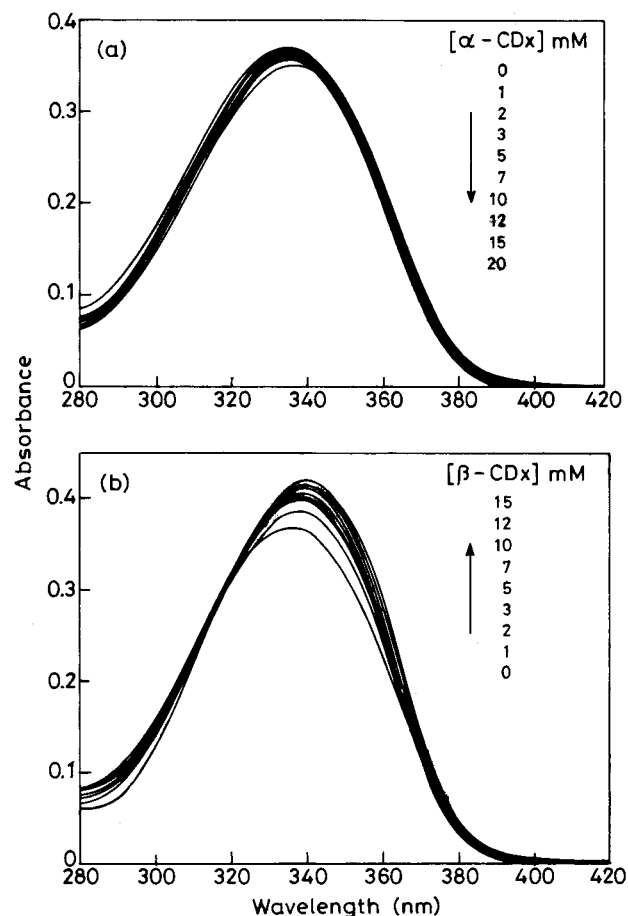
in some other solvents are complied in Table 1. No changes are observed in the long-wavelength (LW) absorption maximum in α-CDx, whereas in β-CDx the LW absorption maximum is red shifted by 5 nm in comparison to that in water. The molecular extinction coefficient is slightly decreased in α-CDx, whereas it increases slightly in β-CDx. The changes in the absorbances are due to the encapsulation of DMAPPI into CDx and are attributed to the detergent action of CDxs, as observed by others also.[43,44] The full width at half the maximum height (fwhm) observed in the LW absorption band in α-CDx, β-CDx, and water are at 5190, 5070, and 5350 cm⁻¹, respectively. No definite isosbestic point is observed in α-CDx, whereas the absorption spectra of DMAPPI in varying concentrations of β-CDx show the presence of an isosbestic point at 319 nm.

3.1.2. Fluorescence Spectrum. Figure 2 depicts the fluorescence spectra of DMAPPI in cyclohexane, water, and aqueous solutions of α-CDx (20 mM) and β-CDx (15 mM) at pH 9.5 and using λ_{exc} 350 nm. The relevant data along with similar results in some other solvents are compiled in Table 1. Similar to that in polar/protic solvents, dual fluorescence is also observed both in α-CDx and β-CDx. The short-wavelength (SW) and LW band maxima are blue shifted by 17 and 45 nm, respectively, when compared to those in aqueous medium; the ϕ_{fl} of the SW and the LW bands increased by a factor of 6 and 43, respectively, for 15 mM concentration of β-CDx at λ_{exc} = 350 nm. Similar changes are also observed in 20 mM α-CDx, but their magnitudes are small compared to β-CDx. The other noticeable feature of emission spectra of DMAPPI in CDxs is that vibrational structure observed in the SW emission band in cyclohexane is absent and the SW emission in CDxs corresponds to either methanol or methanol/water mixture environments.

TABLE 1: Absorption Band Maxima (λ_{max}^{ab}, nm), log ϵ_{max}, the Fluorescence Band Maxima (λ_{max}^{ab}, nm), Fluorescence Quantum Yields (ϕ_{fl}) of Both the Bands, Lifetimes (τ, ns), Radiative Rate ($k_r \times 10^8$ s^{-1}) and Nonradiative Rate ($k_{nr} \times 10^8$ s^{-1}) of the Neutral and the Monocation of DMAPPI in Different Environments (λ_{exc} = 350 nm; [β-CDx] = 15 mM, [α-CDx] = 20 mM)

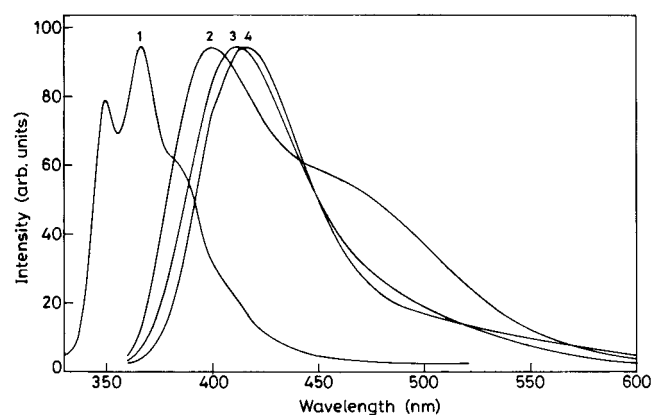| solvent	λ_{max}^{ab} (log ϵ_{max})	λ_{max}^{fl} (ϕ_{fl}) N	TICT	τ_N	τ_T	k_r^N	k_{nr}^N	k_r^T	k_{nr}^T
cyclohexane	327	350, 367, 384 (0.57)							
acetonitrile	335 (4.45)	391 (0.69)		0.96		7.2	3.2		
1-propanol	339 (4.40)	393 (0.76)		1.30		5.8	1.8		
methanol	341 (4.47)	398 (0.22)	475 (0.067)	0.35	1.85	6.2	2.3	0.36	5.1
water (pH 9.5)	335 (4.37)	414 (0.014)	505 (0.003)						
α-CDx(pH 9.5)	335 (4.34)	407 (0.026)	490 (0.009)						
β-CDx (pH 9.5)	340 (4.43)	397 (0.085)	460 (0.129)	0.54	1.74	1.6	16.9	0.74	5.0
methanol (0.001 M H$_2$SO$_4$)	370	413 (0.022)	516 (0.014)						
water (pH 4.0)	368	416 (0.003)	525 (0.0007)						
α-CDx(pH 4.0)	368	416 (0.0029)	510 (0.00097)						
β-CDx (pH 4.0)		408 (0.003)	492 (0.025)		0.44				

Figure 2. Fluorescence spectrum of neutral DMAPPI in (1) cyclohexane, (2) 15 mM aqueous β-CDx, (3) 20 mM aqueous α-CDx, and (4) water. pH 9.5.

TABLE 2: Fluorescence Band Maxima (λ_{max}^{ab}, nm), Fluorescence Quantum Yields (ϕ_{fl}) of Both the Bands of Neutral DMAPPI When Excited at 310, 330, and 350 nm in Water, 15 MM β-CDx, and 20 mM α-CDx ([DMAPPI] = 1.6 $\times$ 10^{-5} M, pH = 9.5)

medium	λ_{max}^{ab}	$\lambda_{exc} = 310$ N	TICT	$\lambda_{exc} = 330$ N	TICT	$\lambda_{exc} = 350$ N	TICT
water	335	414 (0.012)	505 (0.003)	415 (0.010)	505 (0.003)	416 (0.011)	505 (0.0027)
α-CDx	335	409 (0.025)	490 (0.009)	410 (0.023)	490 (0.0078)	411 (0.022)	490 (0.008)
β-CDx	340	397 (0.080)	460 (0.129)	398 (0.072)	460 (0.121)	399 (0.078)	460 (0.122)

The fluorescence spectra of DMAPPI in 20 mM α-CDx and 15 mM β-CDx at pH 9.5 were also studied by exciting at 310, 330, and 350 nm. The relevant data are compiled in Table 2. The fluorescence band maxima of both the bands were independent of λ_{exc}, as observed in aqueous medium. This clearly suggests that both the emissions are occurring from their most relaxed states and the relaxation times of the environments around DMAPPI are shorter than the radiative lifetimes. Unlike alcoholic solvents, the fwhm of the SW emission in β-CDx decreases and that of the TICT band increases with an increase in λ_{exc} (Table 3). The former is less than that observed in methanol at each λ_{exc}. Similar fwhm data in α-CDx for the TICT band could not be obtained because of the uncertainties involved in their band shapes.

The fluorescence excitation spectra were recorded at different emission wavelengths in the range 380−520 nm in aqueous medium, at 20 mM of α-CDx and 15 mM of β-CDx at pH 9.5.

TABLE 3: Full Width at Half the Maximum Height (cm^{-1}) of the Absorption and the Fluorescence Band Maxima Recorded at Different λ_{exc} (nm) and in Different Media

medium	absorption	emission $\lambda_{exc} = 310$ N	TICT	$\lambda_{exc} = 330$ N	TICT	$\lambda_{exc} = 350$ N	TICT
cyclohexane	3690	3440		3430		3450	
acetonitrile	4540	3710		3800		3720	
1-propanol	4020	3330		3810		4000	
methanol	4090	3170		3290		3340	
water	5350			3250			
α-CDx(20 mM)	5190	3900		3870		3740	
β-CDx(15 mM)	5070	2930	4600	2870	4740	2650	4950

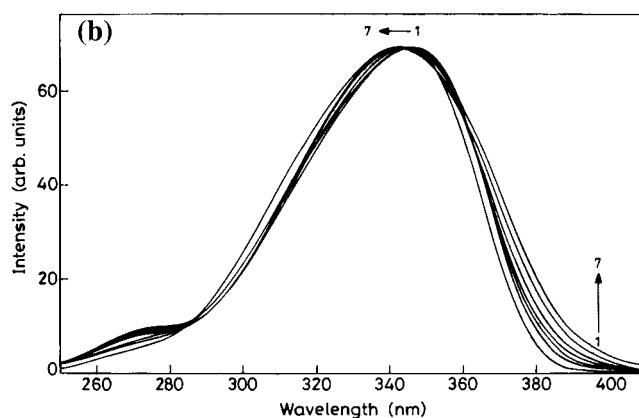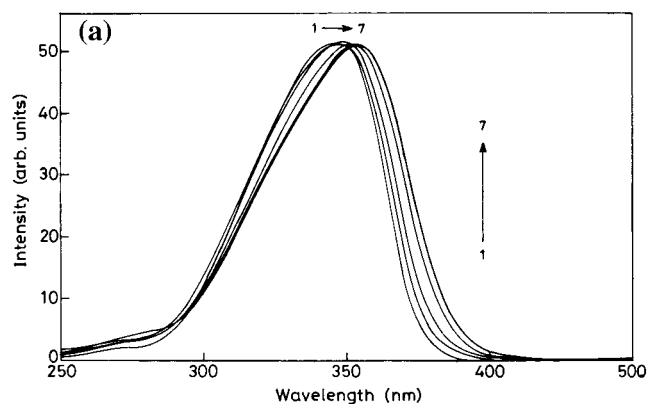**Figure 3.** Fluorescence excitation spectra of DMAPPI in (a) 15 mM aqueous β-CDx and (b) 20 mM aqueous α-CDx. At λ_{em} = (1) 400, (2) 420, (3) 440, (4) 460, (5) 480, (6) 500, and (7) 520 nm.

The excitation spectra in α- and β-CDx are depicted in parts a and b of Figure 3, respectively. The fluorescence excitation band maxima in aqueous medium and β-CDx environments are

Intramolecular Charge Transfer in Cyclodextrins

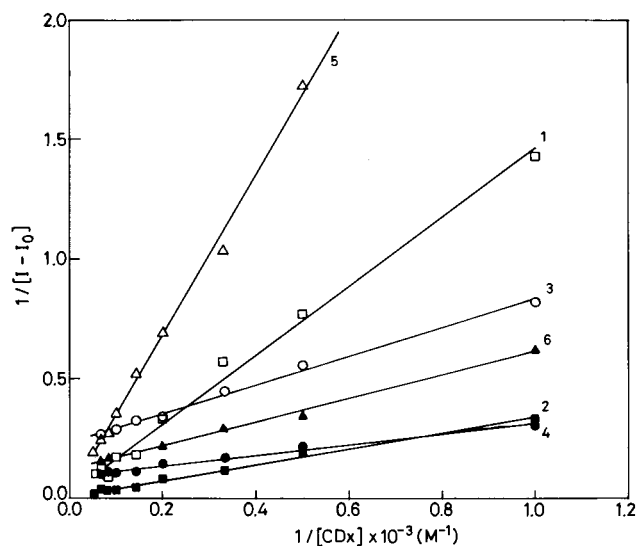*J. Phys. Chem. A, Vol. 104, No. 12, 2000* **2545**

Figure 4. Double reciprocal plot for neural DMAPPI and its mono-cation (MC3) complexes to α-CDx and β-CDx following eq 1 at 298 K. Using normal emission of neutral DMAPPI, (1) α-CDx, (3) β-CDx; using TICT emission of neutral DMAPPI, (2) α-CDx, (4) β-CDx; using TICT emission of the MC3 (5) α-CDx, (6) β-CDx.

slowly red shifted with the increase of λ_{em} up to 440 nm and remained unaltered at $\lambda_{em} > 440$ nm, whereas in the case of α-CDx, fluorescence excitation band maxima are slowly blue shifted with the increase in the λ_{em} up to 440 nm and remain unchanged at $\lambda_{em} > 440$ nm.

The lifetimes of DMAPPI were determined only in 15 mM β-CDx at pH 9.5, as the fluorescence intensities in pure aqueous and 20 nm α-CDx medium were too small to measure the lifetimes in these media. The λ_{exc} was 332 nm and λ_{em} was 397 and 460 nm. The fluorescence decay in each case followed a single exponential and the values so obtained are 0.54 and 1.74 ns, respectively (Table 1), suggesting that the equilibrium is not established between the two states and the rate of formation of TICT state from the locally excited (LE) state is faster than the reverse process. The lifetime of the SW emission increased, whereas that of LW emission decreased slightly when DMAPPI is encapsulated in β-CDx in comparison to those in methanol (0.35 and 1.85 ns). Wherever possible, the values of radiative (k_r) and nonradiative (k_{nr}) rate constants are given in Table 1.

3.1.3. Association Constant. As mentioned earlier, although no clear isosbestic point is observed in the case of α-CDx, one cannot totally eliminate the possibility of the formation of a well defined 1:1 inclusion complex, as the similar results were also observed in p-(N,N-dimethylamino)-[45] and p-(N,N-diethyl-lamino)benzoic acid.[40] Further compared to the absorption intensities, the fluorescence intensities are more sensitive and accurate because of the large emission changes induced by the CDxs. Therefore, the association constants of DMAPPI with β-CDx and α-CDx have been determined using fluorescence intensities and exciting at 319 nm in the former and 360 nm (where the changes observed in the absorption spectra are minimum) in the latter. The Benesi−Hildebrand[46] equation used is

$$\frac{1}{[I - I_0]} = a\left[\frac{1}{[DMAPPI]_0} + \frac{1}{[DMAPPI]_0 K[CDx]_0}\right] \quad (1)$$

where I and I_0 are the emission intensities of DMAPPI with and without CDxs, $[CDx]_0$ and $[DMAPPI]_0$ are the initial concentrations of CDx and DMAPPI, a is a constant, and K is the association constant. Figure 4 represents the double recipro-

TABLE 4: Association Constants (K, M^{-1}) of the Different Species of DMAPPI with CDxs and the pK_a Values of the MC−N Equilibrium of DMAPPI in CDxs

medium	pK_a	λ_{isos} (MC⇌N)	K^a		
			N	TICT	MC3
water	6.45	352			
α-CDx(20 mM)	6.55	352	13 (13.4)	14 (14.3)	4 (4.4)
β-CDx(15 mM)	6.45	355	386 (386.3)	384 (384.2)	246 (246.3)

^{a} Values are obtained from eq 1 and the values in the parenthesis are obtained from eq 2.

cal plot of $1/(I - I_0)$ versus $1/[CDx]_0$. The linear plots show the formation of 1:1 inclusion complex between DMAPPI and both the CDxs. The values of the association constants obtained using the fluorescence intensities of both the bands agree very nicely within error limits (Table 4). The values of K for DMAPPI with β-CDx are larger than those with α-CDx. The value of K can also be calculated using nonlinear least squares regression analysis instead of using the graphical method(eq 1). The equation used for the nonlinear regression analysis[10] is

$$I = \frac{I_0 + aK[CDx]_0}{1 + aK[CDx]_0} \quad (2)$$

The initial values of I_0 and $[CDx]_0$ given to the analysis are the experimental values, and the initial values of K and a given to the analysis are obtained from the Benesi−Hildebrand plot. The fit covered well for all the cases with correlation coefficients $r^2 > 0.95$ (Figure 5). The agreement between the values obtained graphically and theoretically is quite good (Table 4).

3.1.4. Discussion. The spectral characteristics of DMAPPI have been studied in detail.[33] The LW absorption band is red shifted with an increase in polarity and hydrogen bonding capacity of the solvents except water, where it is blue shifted compared to alcoholic solvents. This has been attributed to the fact that the hydrogen bonding at =N$_3$− and =N$_6$− atoms and >NH group makes the PI ring to be planar with the benzene ring and thus increases the conjugation with DMAP ring, whereas the hydrogen bonding at the −NMe$_2$ group in water makes this group nonplanar. The LW emission band is more sensitive than the SW emission to the environments. The increase in the ϕ_{fl} (SW) band with the increase of polarity and hydrogen bonding capacity of the solvents except methanol and water has been attributed to the greater rigidity in the structure of DMAPPI in the S$_1$ state as a decrease in the flexibility in the molecule on excitation to the S$_1$ state decreases the rate of nonradiative decay rate;[47] that is, the molecule is more planar in the S$_1$ state. This is supported by the fact that the fwhm in the fluorescence spectrum is smaller than that in the absorption spectrum. The LW emission band has been assigned to the TICT band. The lifetimes of both the states are different and this suggests that the equilibrium is not established between these two states. The reverse charge transfer (TICT → LE) is significantly reduced.

On the basis of the above results and considering the results in the present study, it may be concluded that a 1:1 inclusion complex is formed between DMAPPI and α-CDx and β-CDx. This is based on the following observations. The ground state geometry of DMAPPI was optimized using the AM1 method[48] (QCMP 137 MOPAC 6/PC). The vertical distance between H$_{29}$ and H$_{32}$ is 4.1 Å and that between H$_{19}$ and H$_{21}$ is 5.1 Å. The horizontal distance between H$_{20}$ and N$_1$ is 5.2 Å, whereas between H$_{27}$ and N$_3$ it is 7.1 Å. Considering the shape and the dimensions of DMAPPI and β-CDx, DMAPPI can enter β-CDx lengthwise in two ways (parts a and b of Scheme 2). If the
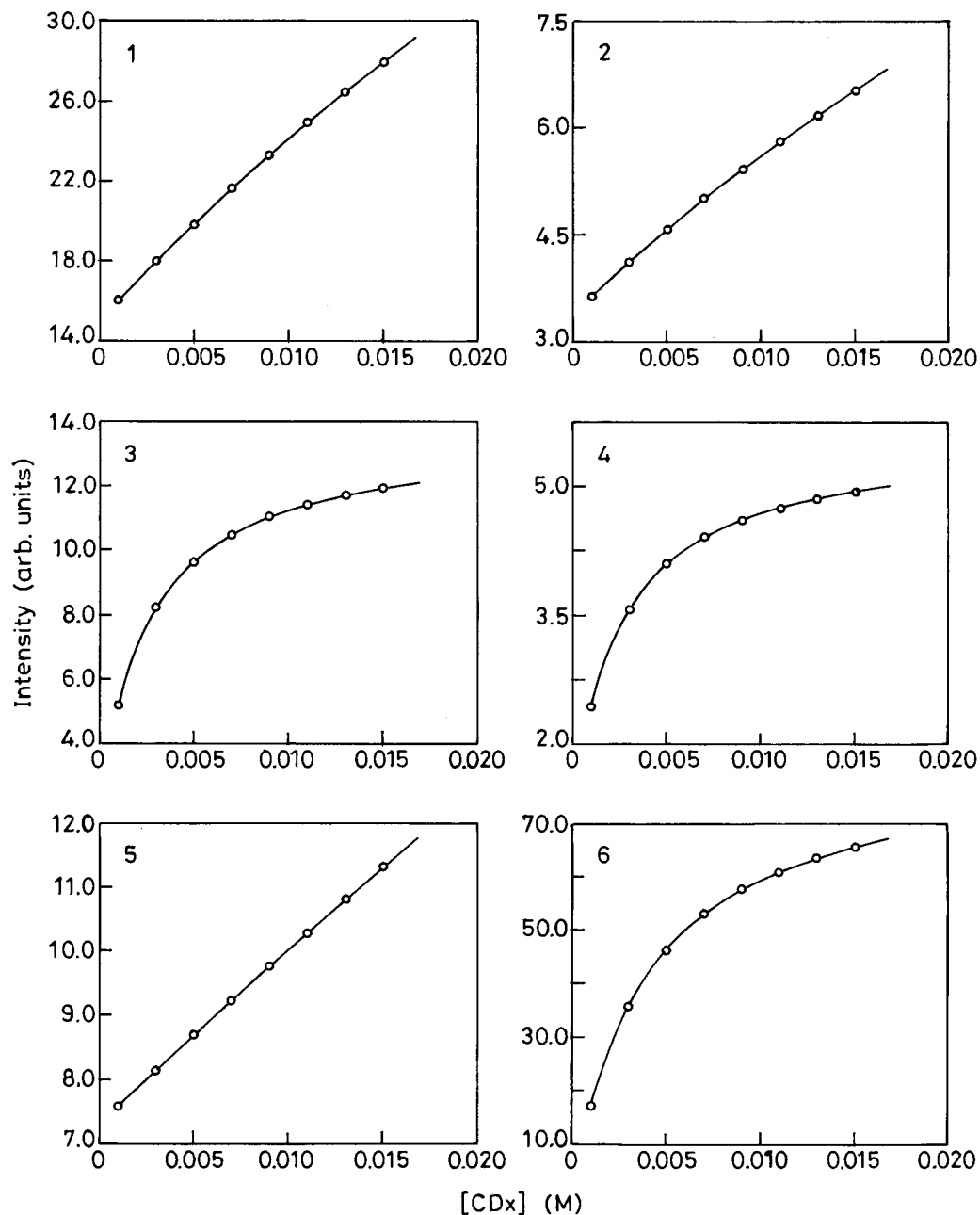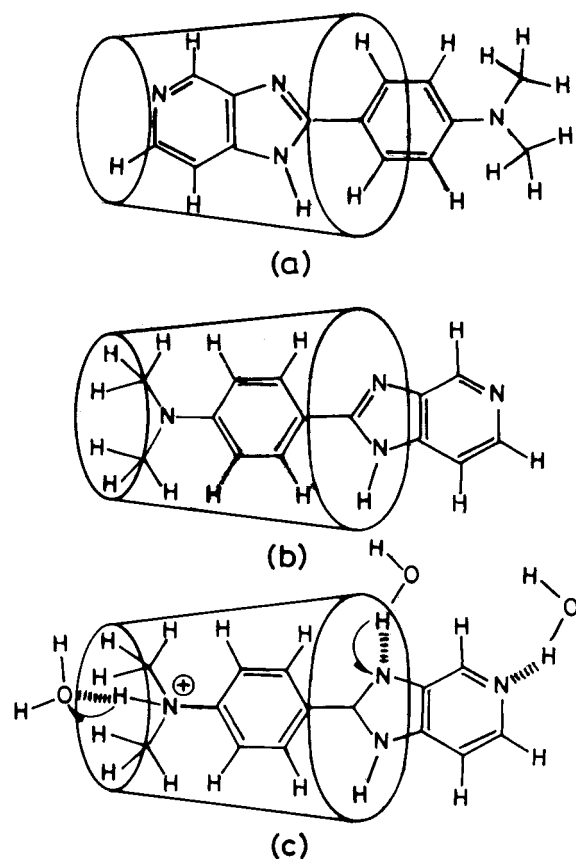
Figure 5. Plot of fluorescence intensities (I) versus [CDx] for DMAPPI complexes to CDx. Using normal emission of neutral DMAPPI, (1) α-CDx, (3) β-CDx; using TICT emission of neutral DMAPPI, (2) α-CDx, (4) β-CDx; using TICT emission of the MC3 (5) α-CDx, (6) β-CDx.

inclusion complex is formed as shown in Scheme 2a, the $-NMe_2$ group will be present in the bulk water phase and will experience the similar kind of solvation at the $-NMe_2$ group as experienced in the bulk water, whereas the hydrogen bonding interactions at $=N_3-$ and $=N_6-$ atoms will be absent. This kind of geometry will lead to the blue shift in the absorption spectrum of DMAPPI when compared with that in water. The results, observed in the Table 1, thus establish that the inclusion complex formed between DMAPPI and β-CDx is as shown in Scheme 2b and is substantiated by the following observations. (i) The $-NMe_2$ group is buried in the hydrophobic cavity, and thus the bulk water is not available to solvate it. This would eliminate the solvation shell around the $-NMe_2$ group and thereby cause a red shift in the absorption spectrum and the blue shifts in both the emission bands. (ii) An increase is observed in the ϕ_{fl} of both the bands. This means that the LE state is less flexible in β-CDx in comparison to that in protic solvents and is substantiated by the fwhm in β-CDx, which is

less than that in protic solvents (Table 3). In other words $=N_3-$ and $>NH$ group are strongly hydrogen bonded to the water molecules at the interface and/or to the secondary hydroxyl protons, leading to the planarity of the PI ring and benzene ring. Whereas, in the case of the TICT band, it is well established that the energy barrier for the TICT process decreases with increase of polarity of the solvents.[35,36] This means that the fluorescence intensity of the A band should decrease as the polarity of the environments decreases. The blue shifts observed in the emission of the A band confirms that the β-CDx cavity is less polar than water. The enhancement in the A band emission in β-CDx is due to the decrease in the dipole$-$dipole interactions between the environment in β-CDx and the TICT state. Because of this, the energy gap between the TICT state and the Franck$-$Condon ground state or the low lying triplet state will increase. The increase in the energy gap between the TICT state and the low-lying triplet/ground state decreases the rate for the nonradiative process.[49] The other factor for the

SCHEME 2

(a)

(b)

(c)

Figure 6. Effect of pH on the absorption spectrum of DMAPPI (a) in 20 mM α-CDx and (b) in 15 mM β-CDx.

enhancement of the TICT emission is the increase in the rigidity of the molecule (see below). (iii) Observation of a similar pK_a value for the protonation of $=N_6-$ atom and the spectral characteristics of the MCs in β-CDx and the bulk water (see later). Single exponential decay at both the emission band maxima and large values of the association constants do suggest the presence of only one kind of inclusion complex between DMAPPI and β-CDx. The large values of the association constant imply that DMAPPI is tightly embedded in the β-CDx cavity.

It is clear from Figure 2 that the SW emission band of DMAPPI is very different in CDxs solutions as compared to that in cyclohexane. This shows that DMAPPI does not experience a nonpolar environment in the CDxs cavity. Although the fluorescence quantum yields of both the bands in β-CDx are different from those in methanol, the band maxima are quite close to those in methanol. In other words, the environment in the β-CDx cavity may be assumed to be close to the methanol polarity. Similar results have also been observed by many regarding the polarity of the β-CDx cavity.[11] Further, the large increase in the fluorescence intensity of A band in β-CDx suggests that the free rotation of −NMe₂ group is still possible in the β-CDx cavity. Considering that the TICT emission was observed in solid matrices and/or under high pressure,[50] it can be considered that the restriction on the increased viscosity in the β-CDx cavity does not forbid the formation of the TICT state. It may thus be mentioned that the formation of the TICT state is dependent more on the polarity of the medium rather than on the free motion (e.g., viscosity), as observed in number of molecules.[11,34,35,49,50]

The observation of TICT emission in β-CDx suggests that the hydrogen bonding of the solvents with the donor group (−NMe₂) does not, whereas that with acceptor (=N− atoms
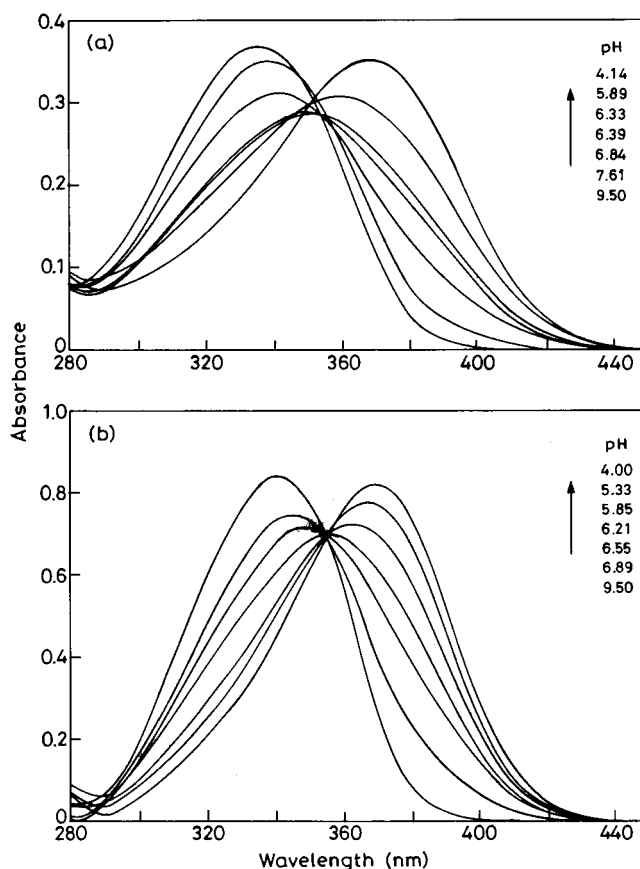
and >NH group of PI ring) does, play the major role in the formation and stabilization of the TICT state. This is because: (i) the −NMe₂ group is buried inside β-CDx cavity (Scheme 2b) and not able to form hydrogen bonds either with the proton of the hydroxyl rim of the shorter cavity nor with water molecules at the interface and (ii) the $=N_3-$ atom and >NH group of the PI ring are held together by the hydrogen bonding of the secondary hydroxyl rim and/or by that of the bound water molecules in the interface more tightly than the free water molecules. This will increase the planarity of the PI ring with the benzene ring and facilitate the flow of charge. This is substantiated by the enormous increase in the TICT emission (43 times that of water) and the decrease in the fwhm of the SW emission of DMAPPI in the β-CDx cavity compared to that in aqueous medium (Table 3).

3.2. Spectral Characteristics of the Monocations. *3.2.1. Absorption Spectrum.* The aborption spectrum of DMAPPI has been studied in 15 mM β-CDx and 20 mM α-CDx aqueous solutions in the pH range 4−9.5. The relevant data are compiled in Table 1, and the spectra are shown in parts a and b of Figure 6, respectively. The presence of an isosbestic point (∼353 nm, sharper in β-CDx in comparison to that in α-CDx) in both the media suggests the presence of equilibrium between the moncation and neutral (MC−N) species. No change is observed either in band maximum or in the absorbance at 368 nm of the MC in α-CDx, whereas the absorption maximum of the MC is red shifted by 2 nm and slight increase (0.045 unit) in the absorbance is observed at 370 nm when dissolved in β-CDx and compared to those in aqueous medium. pK_a values for the MC−N equilibrium determined in α-CDx and β-CDx are similar to each other, as well as obtained in aqueous medium (Table 4). Similar to the absorption spectrum of the neutral DMAPPI,
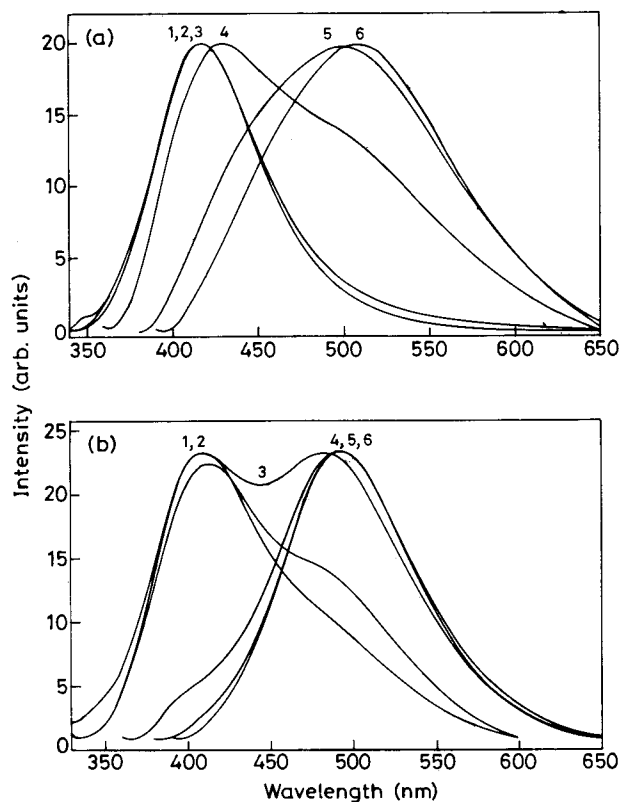
Figure 7. Normalized fluorescence spectrum of MCs of DMAPPI (pH 4.0) (a) in 20 mM α-CDx and (b) in 15 mM β-CDx. λ_{exc} = (1) 310, (2) 320, (3) 330, (4) 350, (5) 370, and (6) 380 nm.

Figure 8. Normalized fluorescence excitation spectrum of MCs of DMAPPI (pH 4.0) at different emissions (a) in 20 mM α-CDx and (b) in 15 mM β-CDx. λ_{em} = (1) 400, (2) 420, (3) 440, (4) 480, (5) 500, (6) 520, and (7) 540 nm.

no clear isosbestic point is observed in the absorption spectrum of the MC when α-CDx concentration is varied, whereas in β-CDx, an isosbestic point is observed in the absorption spectrum of the MC at 385 nm (not shown).

3.2.2. Fluorescence Spectrum. The fluorescence spectra of the MCs of DMAPPI have been studied in 15 mM β-CDx (pH 4.0) with λ_{exc} in the range of 310–380 nm. Dual fluorescence is observed as shown in Figure 7b; that is, 408 nm is the intense emission band and 492 nm is the shoulder when λ_{exc} is 310, 315, and 320 nm, whereas the fluorescence intensity of the 408 nm band keeps on decreasing and that of 492 nm band keeps on increasing as λ_{exc} increases. In comparison to the results in aqueous medium, the SW and LW emission bands in 15 mM β-CDx are blue shifted by 8 and 33 nm, respectively. The fluorescence quantum yield of the SW emission remains unchanged, whereas that of the LW emission increases by a factor of 36 in comparison to those in water. On the other hand, the fluorescence quantum yield of the SW emission in β-CDx decreased by a factor of ~13 and that of the LW emission increased by a factor of ~2 in comparison to those in methanol.

The fluorescence excitation spectra of the MCs in 15 mM β-CDx at pH 4 were also recorded at different λ_{em} and are shown in Figure 8b. Unlike in the absorption spectrum, the 315 nm is the main peak and 377 nm is a shoulder in the fluorescence excitation spectra with λ_{em} in the range 400–440 nm, whereas only one peak at 377 nm with a long tail toward the blue side is noticed when fluorescence excitation spectra are recorded with λ_{em} from 460 to 540 nm. The absorption spectrum of DMAPPI at pH 4 and in 15 mM β-CDx, as well as in aqueous medium, resembles more closely the fluorescence excitation spectra recorded in the emission range 460–540 nm. These observations suggest that the absorption spectrum of the species corresponding to 490 nm emission overlaps with that of the species corresponding to 410 ± 5 nm emission and the relative
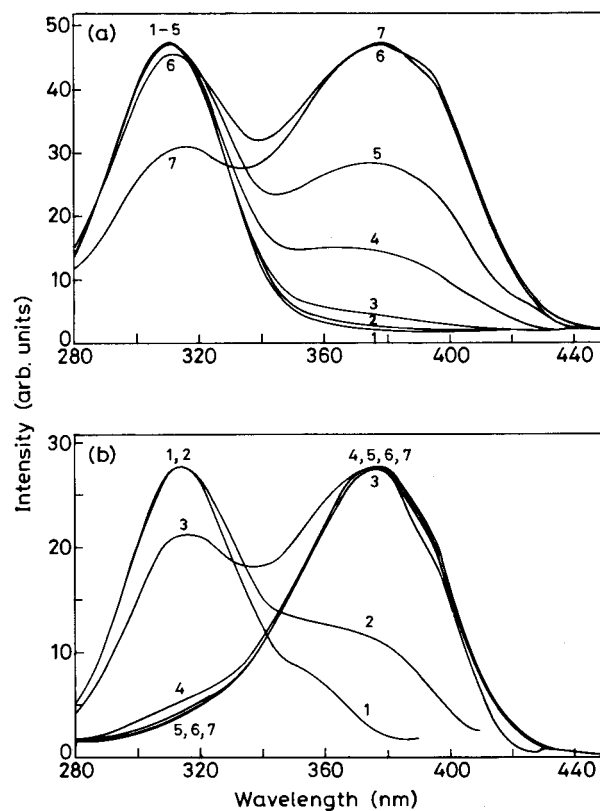
proportion of the former species is larger than the latter in the S_0 state. Further the absorption spectrum of DMAPPI consists of two species. On the basis of the earlier results,[34] the 315 nm band can be assigned to MC1 and the 377 nm band to MC3.

The fluorescence spectra of MCs of DMAPPI were also recorded at λ_{exc} = 310 and 385 nm at different concentrations of CDxs. Parts a and b of Figure 9 represent these changes in β-CDx. These two wavelengths were such that the changes observed in absorption spectra of the MCs were either minimum or represent isosbestic points. From Figure 9a, it is clear that at λ_{exc} = 310 nm the fluorescence intensity of the 416 nm emission band increases slightly up to 3 mM β-CDx and then nearly remains invariant up to 15 mM β-CDx, whereas that of the 490 nm band keeps on increasing with increasing β-CDx concentration (inset of Figure 9a). On the other hand, at λ_{exc} = 385 nm (λ_{isos}), only the LW emission is noticed, and its intensity increases with increase in β-CDx concentration. A weak shoulder observed at ~425 nm in water could be due to MC2 rather than because of the normal emission band of MC3. This is because the fluorescence excitation spectra recorded at 420–440 nm exhibit mainly the 310 nm band rather than at 377 nm.

The fluorescence spectra of DMAPPI at pH 4 (MCs) in 20 mM α-CDx were also recorded using λ_{exc} in the range 310–380 nm (Figure 7a). Hardly any change is observed in the λ^{fl}_{max} and the fluorescence quantum yield of the SW emission, but the λ^{fl}_{max} of the LW emission is blue shifted by 15 nm and the ϕ_{fl} is increased by a factor of 1.4 in comparison to the results observed in aqueous medium. The fluorescence excitation spectra of the MCs of DMAPPI in α-CDx were also recorded at emission wavelengths in the range 400–560 nm (Figure 8a). Unlike the fluorescence excitation spectra of the MCs of DMAPPI in β-CDx, only one peak is observed at 310 nm in
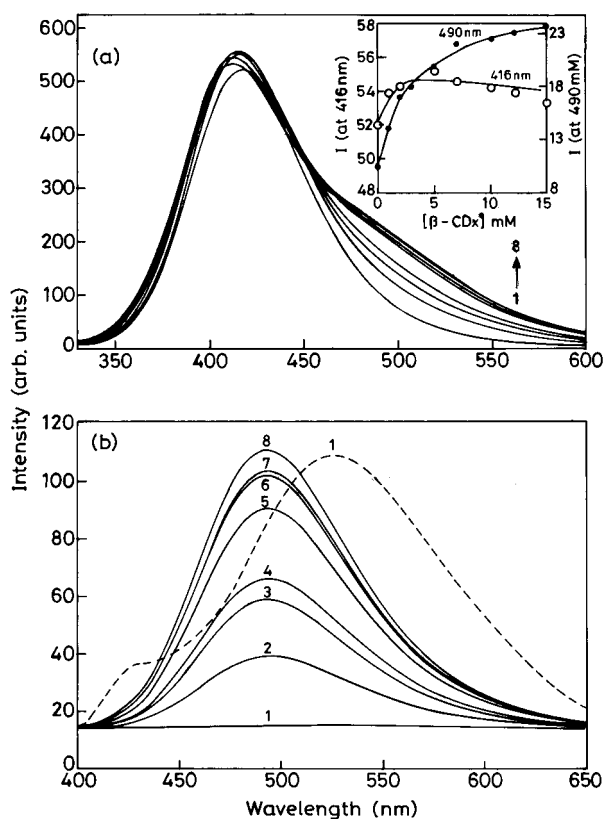
Intramolecular Charge Transfer in Cyclodextrins

J. Phys. Chem. A, Vol. 104, No. 12, 2000 **2549**

Figure 9. Fluorescence spectrum of MCs of DMAPPI (pH 4.0) as a function of β-CDx concentration at λ_{exc}: (a) 310 nm (the inset box shows the plot of intensity (I) of the 416 nm band and 490 nm band versus [β-CDx]) and (b) 385 nm (dotted line shows the spectra in 0 M [β-CDx] in the expanded scale). [β-CDx] = (1) 0, (2) 1, (3) 2, (4) 7, (5) 10, (6) 12, and (7) 15 mM.

the fluorescence excitation spectra of the MCs of DMAPPI in α-CDx when monitored at $400-440$ nm and the second peak at 380 nm starts appearing at the expense of 310 nm peak when $\lambda_{em} \geq 480$ nm. All these behaviors are more close to those observed in aqueous medium[34] rather than to those in β-CDx.

The effect of $\lambda_{exc} = 310$ and 400 nm, respectively, on the fluorescence intensities of the MCs of DMAPPI as a function of α-CDx concentration has also been studied (not shown). In both cases, only one emission band is observed, i.e., ~415 nm in the former and 510 nm in the latter case. Further, only a slight decrease is observed in the 415 nm emission band, whereas an increase in the emission intensity is noticed in 510 nm band.

3.2.3. Association Constants of the MC3. The changes observed in the absorption spectra and the 415 nm emission band were so small that the association constants of the MC3 were determined using eq 1 (Figure 4) and eq 2 (Figure 5) and the changes in the LW emission band. The values so obtained are compiled in Table 4, and the agreement between the two values is quite good. Similar to the neutral molecule, the association constants of the MC3 with α-CDx (4 M^{-1}) is negligible in comparison to that in β-CDx (246 M^{-1}).

3.2.4. Discussion. DMAPPI possesses three basic centers, and three kinds of MCs can be obtained by protonating the $-NMe_2$ group (MC1), $=N_3-$ atom (MC2), and $=N_6-$ atom (MC3) (Scheme 1). The relative proportions of these MCs in the S_0 state, shown by AM1 calculations and electrostatic potential energy mapping,[34] follow the order MC3 > MC1 > MC2. The spectral characteristics of the MCs of DMAPPI in methanol and water have proved that MC1 and MC3 are formed in the

ground state, whereas MC2 and MC3 are present in the S_1 state. MC2 is obtained by the biprotonic phototautomerism in the S_1 state. This process is obtained when the order of the acidities or basicities of the acidic and basic centers are reversed in the S_1 state as compared to that in S_0 state[51] and the formation of the phototautomer is an excited-state phenomenon. On the other hand, when MC3 is excited at its λ_{max}, the emission band observed was assigned to the TICT band. The absence of the normal fluorescence band of this protonated species (MC3) could be either due to the fact that the intramolecular charge transfer state is less stabilized and a $n_N\pi^*$ state is sufficiently low for favoring an alternative decay pathway such as intersystem crossing to the triplet[52,53] or due to the complete transfer of the MC3 to the TICT state which may be sufficiently lower than the normal state in water or methanol.

On the basis of the above arguments and present results, it is clear that the prototropic species formed in both the CDxs are similar to those observed in aqueous or methanol media. Their spectral characteristics are only changed. The spectral characteristics, the values of association constants, and the pK_a value of the MC$-$N equilibrium support our earlier conclusion drawn in section 3.1.4 that DMAPPI forms inclusion complex with β-CDx as shown in Scheme 2b. This conclusion is supported by the following arguments. (i) If DMAPPI molecule would have formed an inclusion complex with β-CDx, as shown in Scheme 2a, both the $=N-$ atoms would have been buried in the nonpolar cavity and situated in such a way that both the $=N-$ atoms would have been away from the hydrogen bonding network at the primary or the secondary hydroxyl rim, making it inaccessible to the attack of the proton. In other words, the pK_a value of the MC$-$N equilibrium would have been lowered. On the other hand, in the case of the other inclusion complex, as shown in Scheme 2b, $=N_6-$ is nearly present in the bulk water phase and $=N_3-$ near the larger rim of β-CDx, i.e., easily accessible to the attack of proton. Nearly similar values of pK_a for the MC$-$N equilibrium confirm the presence of the inclusion complex with β-CDx as shown in Scheme 2b. (ii) Similar to aqueous medium, the normal emission from MC3 is also absent in β-CDx. A similar behavior is also observed when the prototropic reactions of DMAPPI were studied in the ionic (sodium dodecylsulfate and cetyltrimethylammonium bromide) and nonionic (triton X-100) micelles.[54] The presence of water molecules is established from the fluorescence quenching of the fluorophore buried in the core of the micelles by water-soluble quenchers[55] and thus may be involved in hydrogen bonding interactions with the prototropic species. It proves the point that the water molecules present near the rim of the β-CDx are also involved in forming the hydrogen bonding with $>$NH and/or $=N-$ moieties. On the other hand, our study in pure AOT[54] dissolved in *n*-heptane with water content (w_0) zero has substantiated that the emission was only observed from the normal fluorescence state of MC3 at 450 nm and the 450 nm emission band was continuously red shifted to 492 nm emission band with increase of water-to-surfactant ratio w_0. The former situation represents the dielectric constant equal to ~5[56] and deprives the medium of forming hydrogen bonding with the PI ring, whereas in the latter situation, water molecules are available for hydrogen bonding. (iii) As mentioned earlier, the 412 nm emission band is due to a phototautomer whose ground state precursor is MC1 (Scheme 1) and formed in the S_1 state by the simultaneous deprotonation of $-NMe_2H^+$ group and protonation of $=N_3-$ atom involving the solvent system. In the case of β-CDx when the MC1 of DMAPPI is encapsulated in β-CDx, it is held together by the hydrogen bonding as shown

in the Scheme 2c. As soon as the MC1 is excited, it gives away its proton to the water molecules toward the shorter end and accepts the proton from the larger end of the β-CDx. A similar behavior is also observed in the enol−keto tautomerism of 7-hydroxyquinoline.[57] (iv) A single-exponential decay observed in the TICT band of MC3 ($\tau = 0.44$ ns, $\chi^2 = 1.05$) suggests that MC3 is occupying a single site. Although the association constant of MC3 with β-CDx suggests that only 80% of MC3 will be encapsulated, qualitatively still it can be assumed that MC3 is nearly present at one site of β-CDx.

In the case of the aqueous solution of α-CDx, the amount of DMAPPI encapsulating in α-CDx, whether in the neutral form or in the cationic form, is very small. This is evident from the absorption spectra, association constants, and the fluorescence data. Further, from the structure of the DMAPPI molecule as well as the diameters of α-CDx's rim, it is clear that −NMe$_2$ group will be present inside the cavity of α-CDx (however small it may be). This is substantiated by the small increase in fluorescence quantum yields and the blue shifts of both the bands in neutral as well of the MC's of DMAPPI in α-CDx when compared to those of water. Although our results have shown that DMAPPI forms a 1:1 inclusion complex with α-CDx, the small value of the association constant and not clear isosbestic point in the absorption spectra do suggest that DMAPPI may be present at more than one site. Since we are not able to measure the lifetime of either the neutral species or the MC, we are not in a position to say anything more than this.

Unlike β-CDx, the λ_{max}^{fl} and the fluorescence excitation spectra for the MC2 in α-CDx are similar to those of aqueous medium. This suggests that MC2, i.e., the MC1 (in the S$_0$ state), is present in the aqueous medium and not in the α-CDx cavity. It is only the small amount of MC3 which is present in α-CDx. This is substantiated by the blue shift and the increase in quantum yield of MC3. Last, from the relative fluorescence intensity ratio of ∼410 nm band to ∼510 nm band (for example, 1.66:1.42:0.23 in water/aqueous α-CDx/aqueous β-CDx at λ_{exc} = 350 nm) it is clear that the relative population of MC1 (therefore, MC2 in the S$_1$ state) decreases while that of MC3 increases in aqueous α-CDx and further to a large extent in aqueous β-CDx as more and more DMAPPI is encapsulated in the nonpolar cavity, thus confirming that CDxs cavities are less polar than water, i.e., less polar MC3 ($\mu_g = 11$ D) will be present in the CDx cavities than MC1 (μ_g 20.7).

4. Conclusions

The above studies reveal the following. (i) Neutral DMAPPI and its MCs form 1:1 complex with β-CDx, as well as with α-CDx, but the association constants for β-CDx complex are very large as compared to α-CDx complex. (ii) In CDxs, the −NMe$_2$ group is buried inside the cavity and the PI ring is present at the interface. Thus, the molecule is held rigidly planar by the hydrogen bonding with the =N$_3$− atom and >NH group of the PI ring with water molecules present at the interface and/ or with the protons of the secondary hydroxyl rim of CDx and = N$_6$− atom with the bulk water molecules. (iii) Observation of the TICT emission with an enormous increase (43 times that of aqueous medium in 15 mM β-CDx) suggests that the hydrogen bonding of the solvent with the donor group does not have a major role in the formation of the TICT state in DMAPPI, but it does play a major role in the dipole−dipole interaction solvation stabilization of the TICT state. (iv) However, the hydrogen bonding of the solvent with acceptor (PI ring) plays a major role in the formation and stabilization of the TICT state by making it more planar with the benzene ring and thereby

facilitating the charge flow. (v) Similar to in aqueous medium, on protonation of DMAPPI, MC1 and MC3 are formed in the S$_0$ state and MC2 and MC3 are formed in the S$_1$ state. But the relative population of MC1 (therefore MC2 in the S$_1$ state) decreases, while that of MC3 increases in aqueous α-CDx and to large extent in aqueous β-CDx.

References and Notes

(1) Bender, M. L.; Komiyana, M. In *Cyclodextrin Chemistry*; Springer-Verlag: New York, 1978.

(2) Saenger, W. *Angew. Chem., Int. Ed. Engl.* **1980**, *19*, 344.

(3) Szejtli, J. In *Cyclodextrins and Their Inclusion Complexes*; Akademiai Kiado: Budapaste, 1982.

(4) Li, S.; Purdy, W. C. *Chem. Rev.* **1992**, *92*, 1457.

(5) Szejtli, J. *Cyclodextrin Technology*; Kluwer Academic Publishers: Dordrecht, 1988.

(6) Saenger, W. *Angew. Chem., Int. Ed. Engl.* **1984**, *19*, 344.

(7) Schiller, R. L.; Lincon, S. F.; Coates, J. H. *J. Chem. Soc., Faraday Trans. 1* **1987**, *83*, 3237.

(8) Sanrame, C. N.; de Rossi, R. H.; Arguello, G. A. *J. Phys. Chem.* **1996**, *100*, 8151.

(9) Yorozu, T.; Hoshim, M.; Imamura, M.; Shizuka, H. *J. Phys. Chem.* **1982**, *86*, 4422.

(10) Roberts, E. L.; Chou, P. T.; Alexander, T. A.; Agbaria, R. A.; Warner, I. M. *J. Phys. Chem.* **1995**, *99*, 531.

(11) Nigam, S.; Durocher, G. *J. Phys. Chem.* **1996**, *100*, 7135 and reference listed there regarding polarity of β-CDx cavity.

(12) Roberts, E. L.; Dey, J. K.; Werner, I. M. *J. Phys. Chem. A* **1997**, *101*, 5396.

(13) Mitra, S.; Das, R.; Mukcherjee, S. *J. Phys. Chem. B* **1998**, *102*, 3730.

(14) Hamai, S.; Kudou. T. *J. Photochem. Photobiol. A: Chem.* **1998**, *113*, 135.

(15) Hamai, S. *Bull. Chem. Soc. Jpn.* **1998**, *71*, 1549.

(16) Hamai, S. *J. Phys. Chem. B* **1997**, *101*, 1705.

(17) Matushita, Y.; Hikida, T. *Chem. Phys. Lett.* **1998**, *290*, 349.

(18) Connors, K. A.; Lipari, J. M. *J. Pharm. Sci.* **1976**, *65*, 379.

(19) Park, H.; Mayer, B.; Wolschamn, P.; Kohler, G. *J. Phys. Chem.* **1994**, *98*, 6158.

(20) Pitchumanni, K.; Vellayappan, M. *J. Inclusion Phenom. Mol. Recognit. Chem.* **1992**, *14*, 157.

(21) Brown, S. E.; Coates, J. H.; Dukworth, P. A.; Lincon, S. F.; Easton, C. J.; May, B. L. *J. Chem. Soc., Faraday Trans.* **1993**, *89*, 1035.

(22) Sanrame, C. N.; de Rossi, R. H.; Arguello, G. A. *J. Phys. Chem.* **1996**, *100*, 8151.

(23) Kano, K.; Tanaka, N.; Minamizono, H.; Kawakita, Y. *Chem. Lett.* **1996**, 925.

(24) Hamai, S.; Satoh, N. *Carbohydr. Res.* **1997**, *304*, 229.

(25) Hensen, J. E.; Pines, E.; Fleming, G. R. *J. Phys. Chem.* **1992**, *96*, 6904.

(26) Dogra, S. K. *Proc. Indian Acad. Sci.* **1992**, *104*, 635.

(27) Mishra, A. K.; Dogra, S. K. *Bull. Chem. Soc. Jpn.* **1985**, *58*, 3587.

(28) Krishnamoorthy, G.; Dogra, S. K. *J. Photochem. Photobiol. A: Chem.* **1999**, *123*, 109.

(29) Dey, J. K.; Dogra, S. K. *Chem. Phys.* **1990**, *143*, 97.

(30) Krishnamoorthy, G.; Dogra, S. K. *Chem. Phys.* **1999**, *243*, 45.

(31) Dey, J. K.; Dogra, S. K. *Bull. Chem. Soc. Jpn.* **1991**, *64*, 3142.

(32) Dey, J. K.; Dogra, S. K. *J. Phys. Chem.* **1994**, *98*, 3638.

(33) Krishnamoorthy, G.; Dogra, S. K. *Spectrochim. Acta A* **1999**, *55*, 2647.

(34) Krishnamoorthy, G.; Dogra, S. K. *J. Org. Chem.* **1999**, *64*, 6566.

(35) Hicks, J. M.; Vandersall, M. T.; Babarogic, Z.; Einsenthal, K. B. *Chem. Phys. Lett.* **1985**, *116*, 18.

(36) Hicks, J. M.; Vandersall, M. T.; Sitzmann, E. V.; Einsenthal, K. B. *Chem. Phys. Lett.* **1987**, *135*, 413.

(37) Levy, A.; Avnir, D.; Ottolenghi, M. *Chem. Phys. Lett.* **1985**, *121*, 233.

(38) Cazeau-Dubroca, C.; Lyazidi, S. A.; Cambou, P.; Peirigua, A.; Cazeau, Ph.; Pesquer, M. *J. Phys. Chem.* **1989**, *93*, 2347.

(39) Cazeau-Dubroca, C.; Nouchi, G.; Ben Brahim, M.; Pesquer, M.; Gorse, D.; Cazeau, Ph. *J. Photochem. Photobiol. A: Chem.* **1994**, *80*, 125.

(40) Kim, Y. H.; Cho, D. W.; Yoon, M.; Kim, D. *J. Phys. Chem.* **1996**, *100*, 15670.

(41) Cukier, R. L. *J. Phys. Chem.* **1994**, *98*, 2377 and the references listed therein.

Intramolecular Charge Transfer in Cyclodextrins

J. Phys. Chem. A, Vol. 104, No. 12, 2000 **2551**

(42) Middleton, R. W.; Wibberely, D. G. *J. Heterocycl. Chem.* **1980**, *17*, 1757.

(43) Bortulos, P.; Monti, S. *J. Phys. Chem.* **1987**, *91*, 5046.

(44) Santra, S.; Dogra, S. K. *J. Photochem. Photobiol. A: Chem.* **1996**, *101*, 221.

(45) Jiang, Y. B. *J. Photochem. Photobiol. A: Chem.* **1995**, *88*, 109.

(46) Cho, D. W.; Kim, Y. H.; Kang, S. G.; Yoon, M.; Kim, D. J. *J. Chem. Soc., Faraday Trans.* **1996**, *92*, 29.

(47) (a) Mataga, N. *Bull. Chem. Soc. Jpn*. **1963**, *36*, 659. (b) Mataga, N.; Kubato, T. *Molecular Interactions and Electronic Spectra*; Marcel Dekker: New York, 1970.

(48) Dewar, M. J. S.; Zeobish, E. G.; Healy, E. F.; Stewart, J. J. P. *J. Am. Chem. Soc*. **1985**, *107*, 3092.

(49) Nag, A.; Dutta, R.; Chattopadhyay, N.; Bhattacharyay, K. *Chem. Phys. Lett.* **1989**, *157*, 83.

(50) Cazeau-Dubroca, C.; Peirigua, A.; Lyazidi, S. A.; Nouchi, G.; Cazeau, Ph.; Lapouyada, R. *Chem. Phys. Lett.* **1986**, *124*, 110.

(51) Swaminathan, M.; Dogra, S. K. *J. Am. Chem. Soc*. **1983**, *105*, 6223.

(52) Tway, P. C.; Love, L. J. C. *J. Phys. Chem.* **1982**, *86*, 5223, 5227.

(53) Fasani, E.; Abini, A.; Savarino, P.; Viscardi, G.; Barni, E. *J. Heterocycl. Chem*. **1993**, *30*, 1041.

(54) Krishnamoorthy, G.; Dogra, S. K. Unpublished results.

(55) Saha, S. K.; Krishnamoorthy, G.; Dogra, S. K. *J. Photochem. Photobiol. A: Chem.* **1999**, *121*, 191 and references therein.

(56) Belletete, M.; Lachapelle, M.; Durocher, G. *J. Phys. Chem.* **1990**, *94*, 5337.

(57) Garcia-Ochoa, I.; Lopez, M. A. D.; Vinas, M. H.; Santos, L.; Ataz, E. M.; Sanchez, F.; Douhal, A. *Chem. Phys. Lett.* **1998**, *296*, 335.